Supplementary Information for

Reusable Co_xNi_{1-x} dye adsorbents as supercapacitor electrode materials

Haiming Sun[a]‡, Xijia Yang[a]‡, Lishu Zhang[b], Lijun Zhao*[a] and Jianshe Lian*[a]

[a] Key Lab of Automobile Materials, Ministry of Education, College of Materials Science and Engineering, Jilin University, Nanling Campus, Changchun, 130025, P. R. China. E-mail: lijunzhao@jlu.edu.cn; lianjs@jlu.edu.cn; Fax: +86-431-85095876; Tel: +86-431-85095878; +86-431-85095875

[b] Institute of Advanced Materials for Nano-Bio Applications, School of Ophthalmology & Optometry, Eye Hospital, Wenzhou Medical University, 270 Xueyuan Xi Road, Wenzhou, Zhejiang, 325027, PR China.

‡ These authors contributed equally to this work.

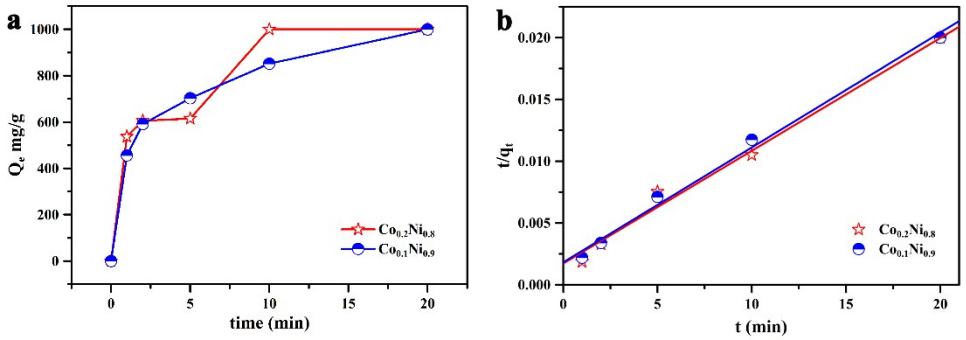

Fig. S1 a) Adsorption isotherm and b) Pseudo-second-order adsorption kinetic for adsorption of CR by the as-synthesized $Co_{0.2}Ni_{0.8}$ and $Co_{0.1}Ni_{0.9}$ binary metallic alloys. (Initial dye concentration 100 mg L^{-1}, pH is about 7.5, temperature 25 ^oC)

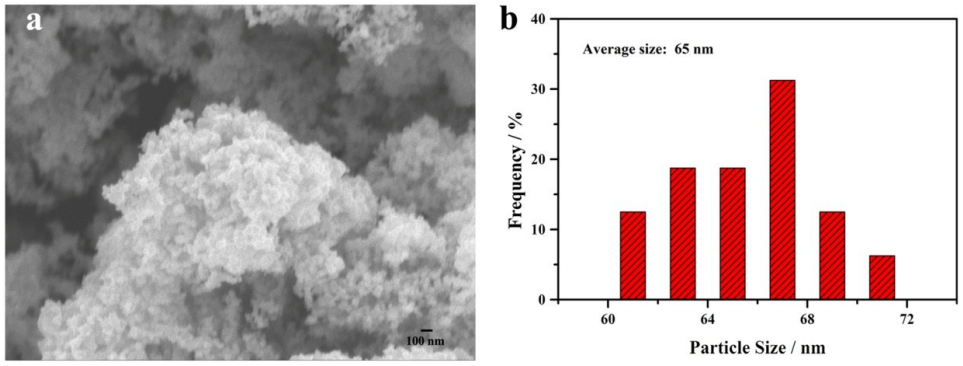

Fig. S2 FE-SEM image and particles sizes distribution of as-synthesized $Co_{0.2}Ni_{0.8}$ alloy without additional treatment. (The particle sizes are calculated by Nano Measurer 1.2).

Table S1 The weight percentage of each element calculated by EDS spectrum.

Element	C	O	S	Co	Ni
wt%	12.63	24.24	1.40	14.66	47.07

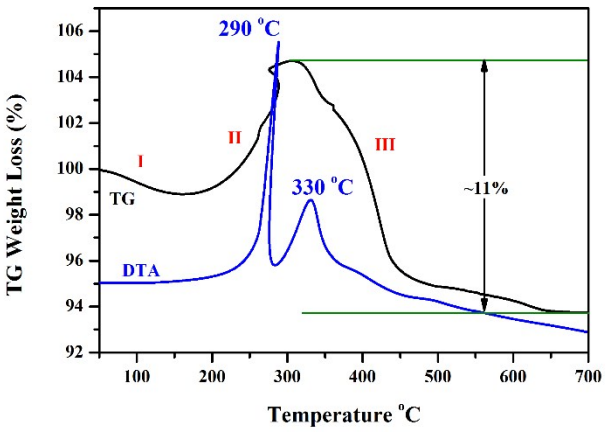

Fig. S3 TG-DTA curves of the M/MO@C-600 composite recorded under air atmosphere (flow rate: 100 mL min^{-1}) from room temperature to 700 °C with a temperature ramp 10 °C min^{-1}.

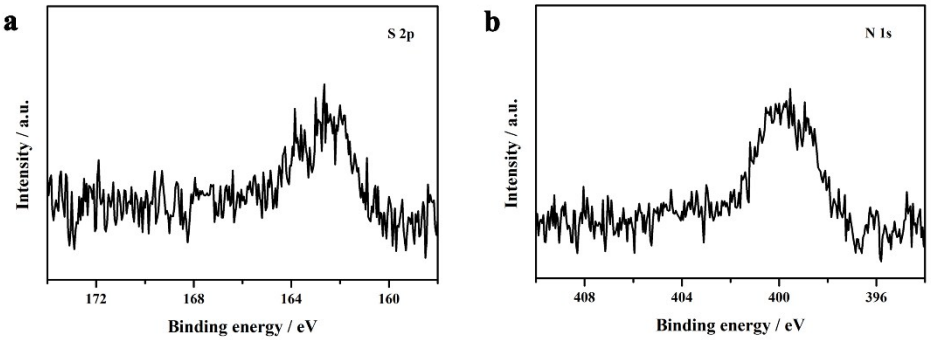

Fig. S4 XPS spectra of a) S 2p and b) N 1s.

Table S2 The atomic percentage of each element calculated by XPS spectrum.

Element	C	O	N	S	Co	Ni
at%	73.94	18.71	0.48	0.71	1.24	4.92

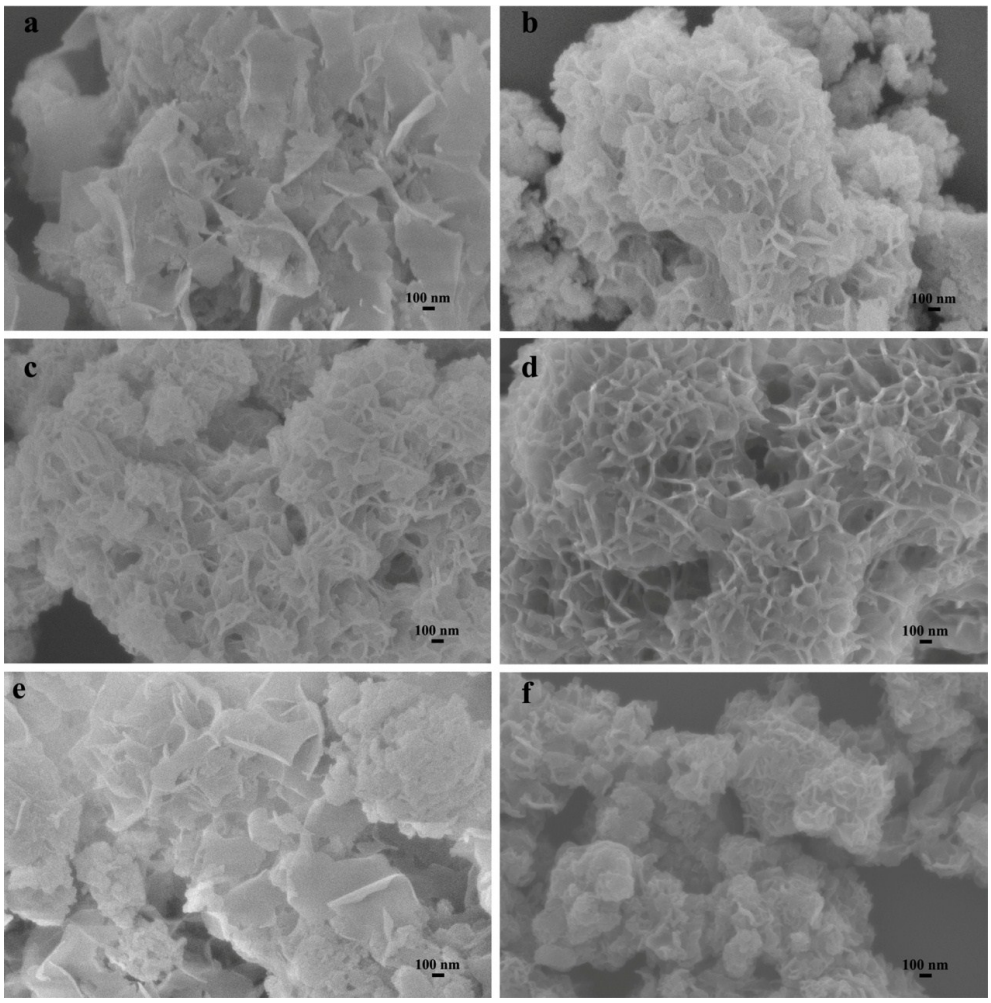

Fig. S5 FE-SEM images of M/MO@C composites with the M constituent of: a) Co, b) $Co_{0.6}Ni_{0.4}$, c) $Co_{0.4}Ni_{0.6}$, d) $Co_{0.2}Ni_{0.8}$ (M/MO@C-600), e) $Co_{0.1}Ni_{0.9}$ and f) Ni. (Calcination temperature: 600 ^{o}C)

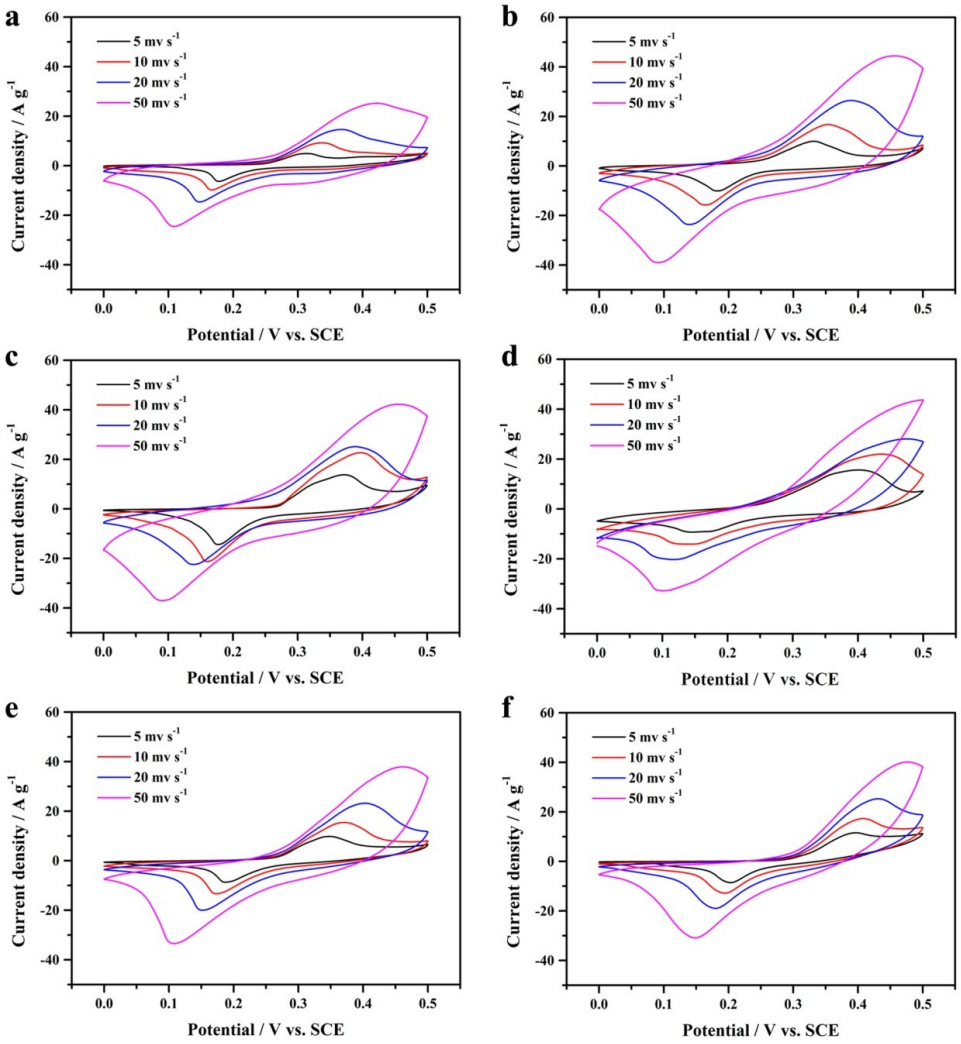

Fig. S6 CV curves of M/MO@C composites with the M constituent of: a) Co, b) $Co_{0.6}Ni_{0.4}$, c) $Co_{0.4}Ni_{0.6}$, d) $Co_{0.2}Ni_{0.8}$ (M/MO@C-600), e) $Co_{0.1}Ni_{0.9}$ and f) Ni. (Calcination temperature: 600 ^{o}C)

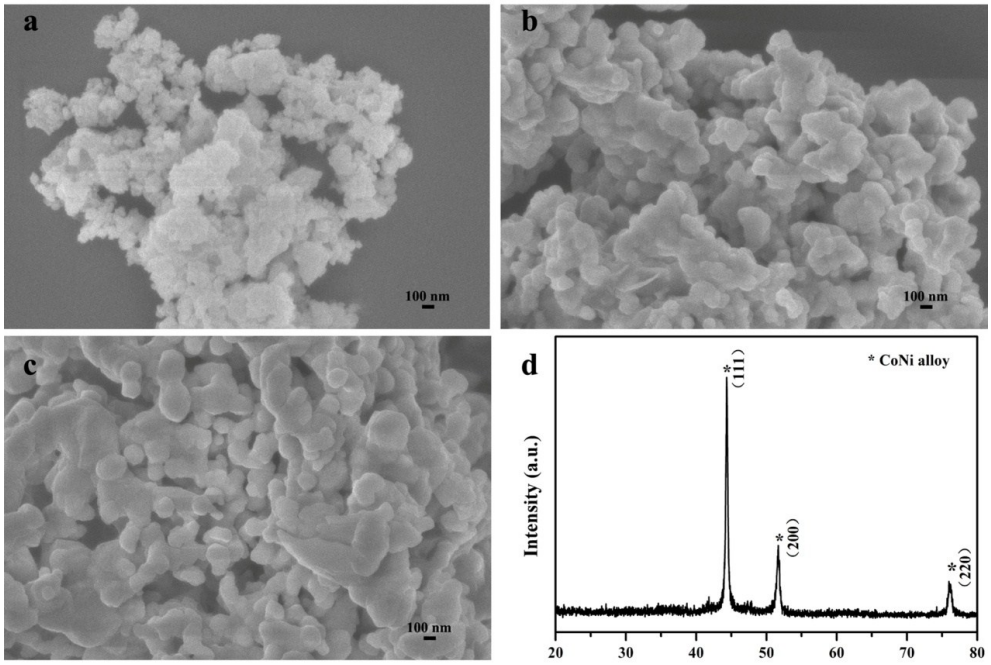

Fig. S7 FE-SEM images of a) M-500, b) M-600, c) M-700; d) XRD profile of M-600.

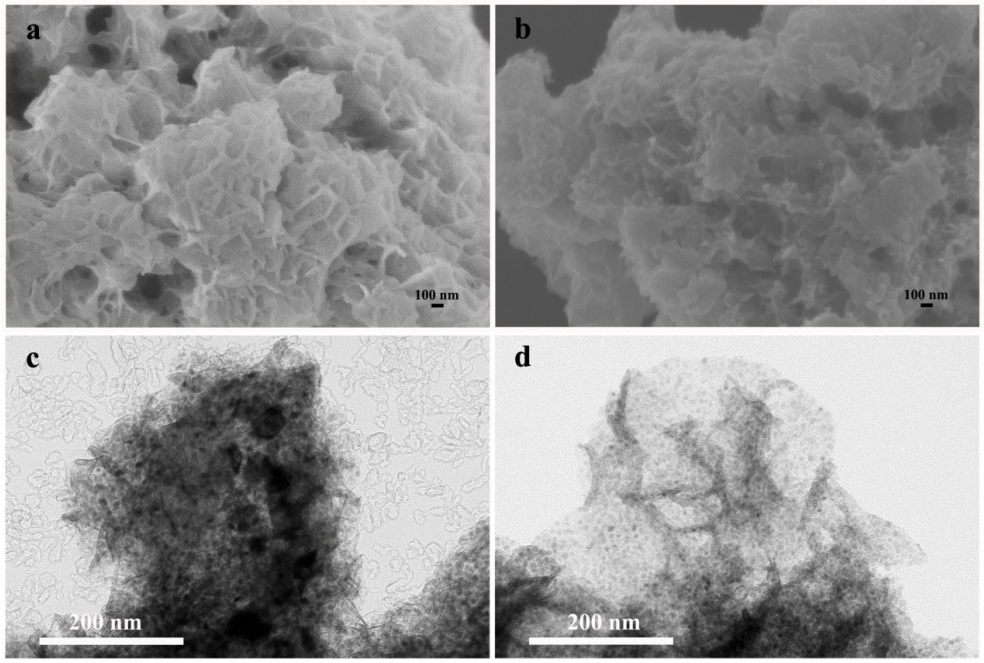

Fig. S8 FE-SEM images of a) M/MO@C-500 and b) M/MO@C-700; TEM images of c) M/MO@C-500 and d) M/MO@C-700.

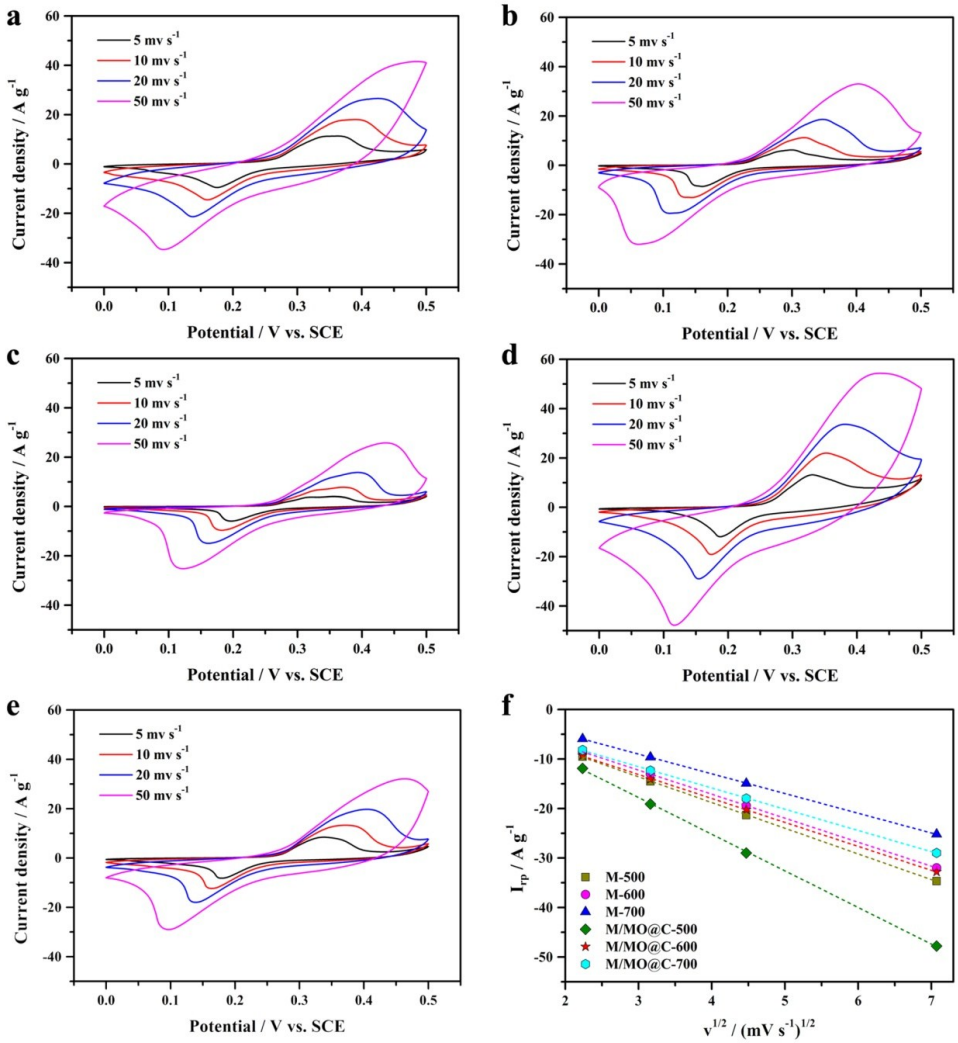

Fig. S9 CV curves of a) M-500, b) M-600, c) M-700, d) M/MO@C-500 and e) M/MO@C-700; f) Corresponding I_{rp}-$v^{1/2}$ plots.

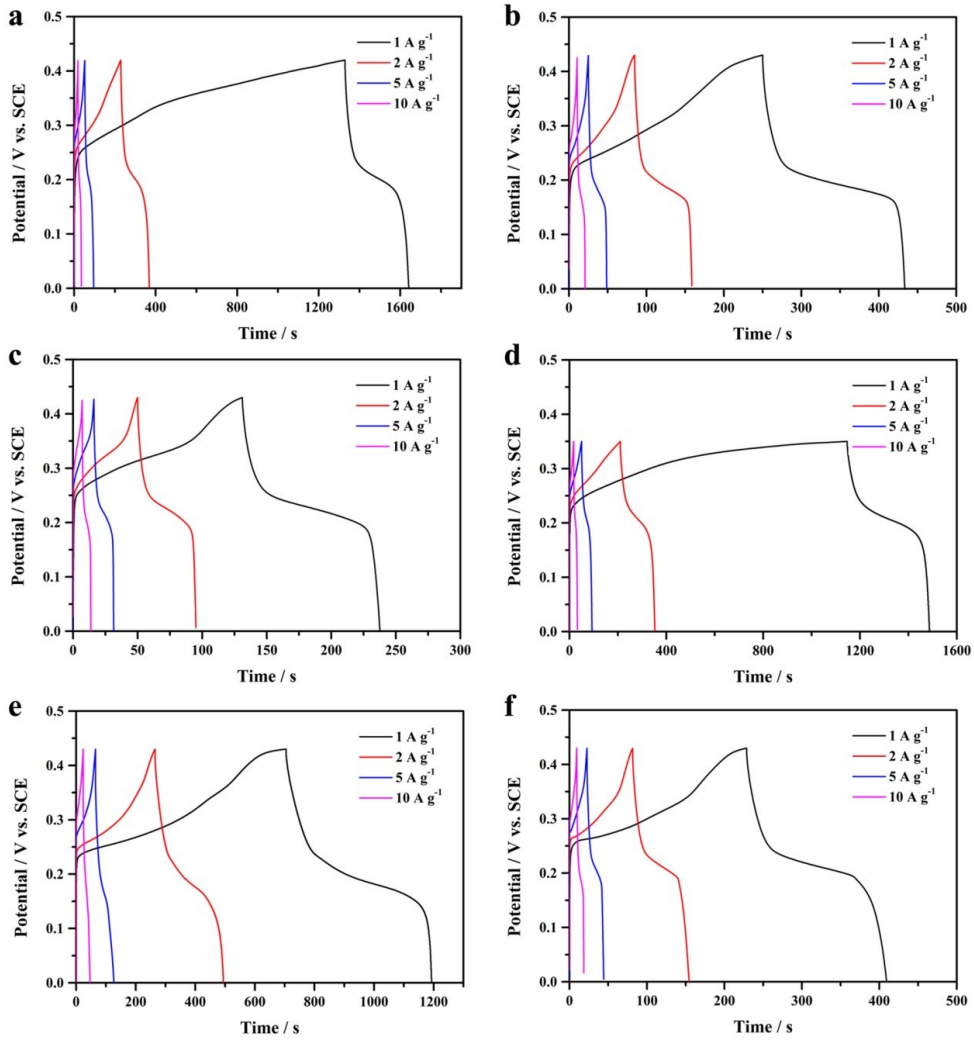

Fig. S10 Galvanostatic charge/discharge curves of a) M-500, b) M-600, c) M-700, d) M/MO@C-500, e) M/MO@C-600 and f) M/MO@C-700.

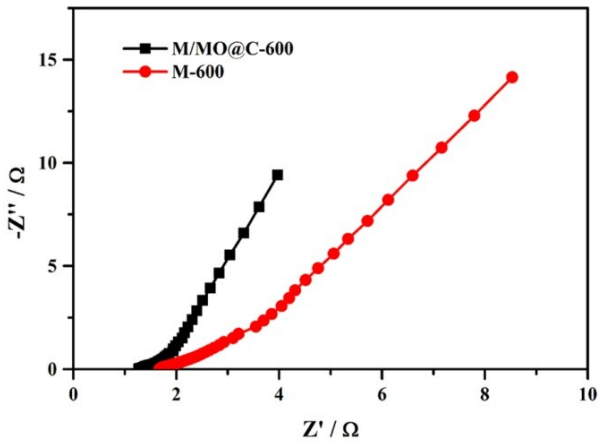

Fig. S11 EIS spectra of the M/MO@C-600 and M-600 composites.

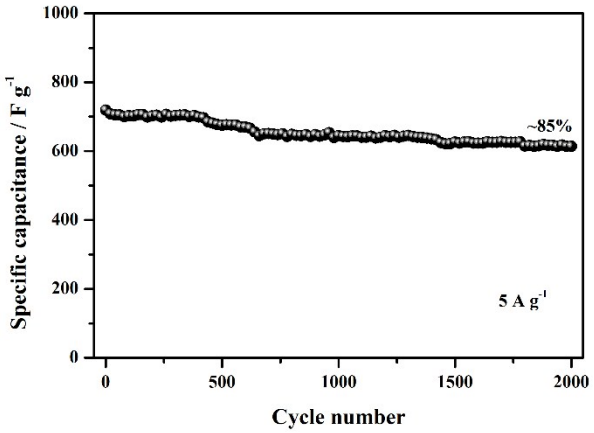

Fig. S12 Cycling performance of M/MO@C-600 composite in the three-electrode system at a current density of 5 A g^{-1}.

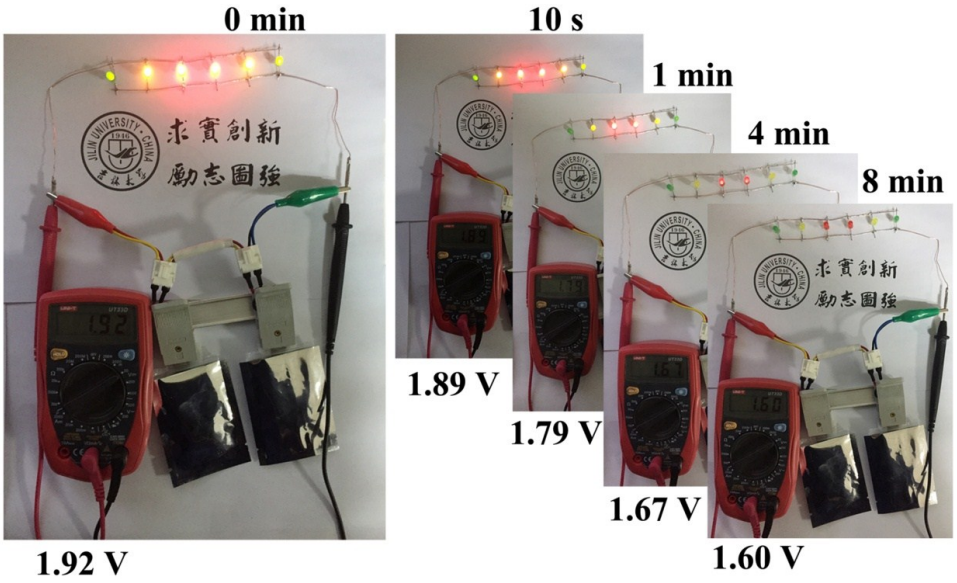

Fig. S13 Time-dependence optical images of two serials connected M/MO@C-600//AC supercapacitors lighten up six parallel connected LED indicators.